

Temporal patterns and drivers of CO₂ emission from dry sediments in a groyne field of a large river

Matthias Koschorreck¹, Klaus Holger Knorr², Lelaina Teichert^{1,2}

¹Department of Lake Research, Helmholtz Centre for Environmental Research – UFZ, Magdeburg, 39114, Germany

²Institute of Landscape Ecology, Westfälische Wilhelms-University, Münster, Germany

Correspondence to: Matthias Koschorreck (Matthias.koschorreck@ufz.de)

Abstract. River sediments falling dry at low water level are sources of CO₂ to the atmosphere. While the general relevance of CO₂ emissions from dry sediments has been acknowledged and some regulatory mechanisms identified, knowledge on mechanisms and temporal dynamics is still sparse. Using a combination of high frequency measurements and two field campaigns we thus aimed to identify processes responsible for CO₂ emissions and to assess temporal dynamics of CO₂ emissions from dry sediments at a large German river.

CO₂ emissions were largely driven by microbial respiration in the sediment. Observed CO₂ fluxes could be explained by patterns and responses of sediment respiration rates measured in laboratory incubations. We exclude groundwater as a significant source of CO₂ because the CO₂ concentration in the groundwater was too low to explain CO₂ fluxes. Furthermore, CO₂ fluxes were not related to radon fluxes, which we used to trace groundwater derived degassing of CO₂.

CO₂ emissions were strongly regulated by temperature resulting in large diurnal fluctuations of CO₂ emissions with emissions peaking during the day. The diurnal temperature – CO₂ flux relation exhibited a hysteresis which highlights the effect of transport processes in the sediment and makes it difficult to identify temperature dependence from simple linear regressions. The temperature response of CO₂ flux and sediment respiration rates in laboratory incubations was identical. Also deeper sediment layers apparently contributed to CO₂ emissions because the CO₂ flux was correlated with the thickness of the unsaturated zone, resulting in CO₂ fluxes increasing with distance to the local groundwater level and with distance to the river. Rain events lowered CO₂ emissions from dry river sediments probably by blocking CO₂ transport from deeper sediment layers to the atmosphere. Terrestrial vegetation growing on exposed

sediments greatly increased respiratory sediment CO₂ emissions. We conclude that the regulation of CO₂ emissions from dry river sediments is complex. Diurnal measurements are mandatory and even CO₂ uptake in the dark by phototrophic micro-organisms has to be considered when assessing the impact of dry sediments on CO₂ emissions from rivers.

1 Introduction

1.1 CO₂ emissions from dry river sediments – significance

Streams and rivers are well known to play an important role in the global carbon cycle. The transport of continental carbon to the ocean is mainly regulated by rivers (Schlesinger and Melack 1981). Moreover, carbon in rivers undergoes transformation processes and can be temporarily stored by means of sedimentation and photosynthesis or released due to biological respiration (Battin et al. 2009). One distinctive feature of rivers is their frequently changing water level. Climate change is expected to further increase the seasonal and the inter-annual variability of rivers and hydrological regimes (Bolpagni et al. 2019; Coppola et al. 2014). In Europe, more frequent and longer-lasting droughts are expected during summers, which lead to low water levels in streams and rivers (Spinoni et al. 2018). Consequently, previously submerged river sediment will be exposed to the atmosphere and influenced by drying (Steward et al. 2012). It has been shown that these exposed sediments can emit high amounts of CO₂ (von Schiller et al. 2014) and may represent a globally relevant carbon source to the atmosphere (Marcé et al. 2019).

1.2 Regulation of CO₂ emissions from dry sediments

While the relevance of CO₂ emissions from dry river sediments has been acknowledged, only little is known about underlying mechanisms and temporal patterns. A recent study identified organic matter content and moisture as common drivers of CO₂ emissions from dry aquatic sediments (Keller et al. 2020). However, high variability prevents the prediction of CO₂ fluxes for particular sites. Case studies showed that CO₂ emissions are affected by temperature (Doering et al. 2011), emergent vegetation (Bolpagni et al. 2017), organic matter (Palmia et al. 2021), water content (Martinsen et al. 2019), or the frequency of

dry-wet cycles (Machado dos Santos Pinto et al. 2020). Although it is known that CO₂ emission from dry sediment may change with time, existing studies are based on single or few measurements. Few studies
55 addressed temporal variability of CO₂ emissions, but nothing is yet known about short term dynamics of
GHG emissions from dry aquatic sediments. Investigating temporal variability of CO₂ fluxes should
provide information about the potential sources of emitted CO₂. Knowing sources of emitted CO₂ from
dry sediments is crucial to be able to model or scale up GHG emissions from these systems.

1.3 Possible sources of CO₂

60 Carbon emissions from desiccated sediments derive from a number of possible biotic and abiotic sources
(Marcé et al. 2019). Microbial respiration is well known to contribute to CO₂ emissions (Weise et al.
2016), similar to soil respiration. Organic matter originating from organic particle sedimentation may be
mineralized to CO₂ or CH₄. It is typically observed that CH₄ emissions from dry sediments are low
indicating that anaerobic mineralization plays a minor role (Marcé et al. 2019).
65 In contrast to respiration, abiotic processes are rarely taken into account as sources of CO₂ (Rey 2015).
Yet, recent findings revealed a spatial variability of CO₂ fluxes from dry river sediments with highest
fluxes near to the river (Mallast et al. 2020). As a possible explanation the authors hypothesized that at
decreasing river water level a groundwater flow gradient towards the river would transport groundwater
to the river (Peters et al. 2006). Groundwater is usually 10 to 100 fold super-saturated with CO₂
70 (Macpherson 2009). Near to the river the thickness of the unsaturated layer approaches zero and CO₂ rich
groundwater reaches the surface sediment where CO₂ would eventually degas.

1.4 Aim of study

Given the uncertainty of the origin of CO₂ emitted from dry river sediments, in this study we aimed to
test the hypothesis of (Mallast et al. 2020) that CO₂ emissions from dry sediments of larger rivers are
75 driven by groundwater degassing. If groundwater was a significant source of CO₂ we hypothesize a only
weak temperature dependence of CO₂ emissions. We applied a combination of automatic high frequency
measurements and detailed studies using a variety of methods to identify the source of CO₂ emissions
from dry sediments at a large German river and to understand their temporal dynamics and drivers.

2 Material and Methods

80 2.1 Study site

The study was conducted at the lowland part of river Elbe, one of the largest rivers in Central Europe with a discharge average of about $559 \text{ m}^3 \text{ s}^{-1}$ at the city of Magdeburg (Weigold and Baborowski 2009). Near Magdeburg, the Middle Elbe can be characterized as a free-flowing lowland river with comparable large floodplains, only regulated by groyne fields. Such groyne fields are the dominant shore type along the
85 German part of the river (Bussmann et al. 2022).

Hence, seasonal water level fluctuations are shaping the different habitats alongside the river, ranging from alluvial forests and pastures to sandy beaches (Scholten et al. 2005). The study site is located near the farm “Apfelwerder” at river km 314 in between two groins and is characterized by a slight slope from the river to the adjoining pasture (52.038398 N, 11.715495 E). Groynes extended about 50 m into the
90 river and distance between groynes was 130 ± 37 m. A sandy beach of about 2 to 5 m with sparse vegetation (*Persicaria lapathifolia*, *Rorippa amphibia*, *Polygonum aviculare*) could be found directly at the river, while the vegetation became denser with distance to the river (Figure S1).

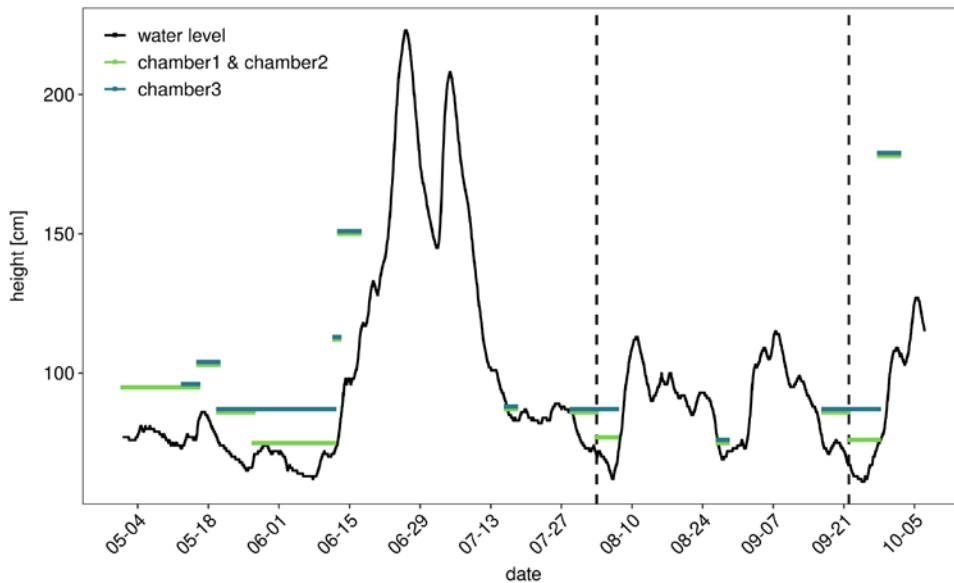
2.2 High frequency measurements

2.2.1 Automatic flux chambers, water table levels, and environmental data

95 To cover the temporal dynamics of CO_2 fluxes three opaque automatic chambers (CFLUX-1 Automated Soil CO_2 Flux System, PP Systems, Amesbury, Massachusetts, USA), were installed (Figure S1). The chambers measured CO_2 fluxes once every hour. Each flux measurement lasted 5 minutes and between flux measurements the chambers were open for 55 min. CO_2 fluxes were calculated from the linear increase of CO_2 during a closure time of 5 minutes. Each chamber was equipped with a soil moisture and
100 temperature probe (Stevens HydraProbe, Stevens Water Monitoring Systems, Portland, Oregon, USA). Due to fluctuating water levels over the summer of 2020 (Figure 1), it was not possible to measure CO_2 fluxes from the sediment continuously over the whole measurement period. The chambers were set up in the periods from May 1st to June 10th, from August 3rd to August 6th, and from September 17th to September 26th; moreover, also during deployment they needed to be moved occasionally. Automatic flux

105 chamber data were discarded when the collar was flooded or the sand was washed away by waves, which resulted in CO₂ concentrations fluctuating around ambient concentration. The final dataset contained 3128 flux measurements.

Because we did not know the exact elevation of our research site, we installed the chambers at defined heights relative to the gauge “Magdeburg Strombrücke” (located 13 km downstream of the study side, 110 zero point of gauge = 39.885 m above mean sea level (WSV 2020)). Therefore, the distance to the river and the height over water level were determined once, along a transect. Out of these parameters, a slope was calculated and afterward used to position the automatic chambers in the field. Positions, where the automatic chambers were placed were related to gauge levels 75, 85 and 95 cm. In other words: When the gauge recorded a water level of e.g. 75, a chamber at the “75 cm position” was located directly above 115 the water line at our research site. The thickness of the unsaturated sediment was calculated as the difference between the height above zero gauge for each chamber and the actual river level. Weather data from the German Weather Service were obtained for the monitoring station Magdeburg 15 km from Apfelwerder (DWD 2020).



120 **Figure 1:** Water level of the Elbe River at gauge “Magdeburg Strombrücke” (13 km downstream) in summer 2020. Colored lines indicate positioning of automatic flux chambers. For example a horizontal line at 95 cm means that a particular chamber was located at the water line when the gauge recorded a water level of 95 cm. Vertical dotted lines indicate intensive sampling campaigns.

2.2.2 High resolution sediment respiration flux transects

To investigate spatial variability, between May and September transects of sediment respiration were measured with a portable soil respiration system (EGM-5 Portable CO₂ Gas Analyser + SRC, PP Systems, Amesbury, Massachusetts, USA) equipped with the same soil moisture and temperature probe as the automatic chambers. On each occasion 12 flux measurements along a 15m long transect from the water upslope were recorded. The opaque chamber was placed on vegetation-free spots to make sure that sediment respiration was measured. At each measuring spot we took note whether plants were growing

130 nearby.

2.3 Detailed sampling campaigns

To closer investigate the mechanisms behind the CO₂ flux two intensive measurement campaigns were carried out on August 4, 2020, and September 23, 2020.

2.3.1 Manual chamber measurements

135 To quantify CO₂ fluxes at different distance to the river and also check for CH₄ emissions, manual chamber
measurements were done in 1 m steps away from the flowing water, along a transect which was
characterized by an uphill slope of ~ 11.5 %. Collars (39 cm diameter) were installed at 4 sites along the
transect a day in advance to minimize disturbance during measurements (Figure S1b). For flux
measurements an opaque chamber ($V = 0.0239 \text{ m}^3$, $A = 0.1195 \text{ m}^2$) equipped with a pressure vent tube
140 was placed on a collar. The concentrations in the chamber were measured every 30 s for ~ 5 minutes with
a multicomponent FTIR gas analyser (DX4000, Gaset Technologies GmbH, Helsinki, Finland). The
FTIR gas analyser continuously measures CO₂, CH₄, and Nitrous oxide (N₂O) with an accuracy of ± 4
ppm CO₂, ± 0.1 ppm CH₄ and N₂O (Gaset Technologies GmbH 2018). Hence, the detection limit of
the CO₂ flux was $\sim 2 \text{ mmol m}^{-2} \text{ d}^{-1}$, while the CH₄ flux was detectable if above $0.12 \text{ mmol m}^{-2} \text{ d}^{-1}$, and
145 N₂O if above $0.2 \text{ mmol m}^{-2} \text{ d}^{-1}$. Fluxes were calculated from the linear increase of the respective gas
mixing ratio (Gomez-Gener et al. 2015) with time using the R package glimr (Keller 2020).

2.3.2 Rn sediment efflux measurements

To assess groundwater degassing ²²²Rn measurements were performed. The geogenic gas ²²²Rn is a
commonly used natural tracer for groundwater influence in aquatic systems and is additionally known as
150 a useful tool to trace the origins of CO₂ (Cook and Herczeg 2000). Therefore, ²²²Rn concentrations and
fluxes were measured with a portable radon detector (RAD7 Radon Detector, DURRIDGE, Billerica,
Massachusetts, USA) to determine the groundwater influence on CO₂ fluxes from dry river sediments.
The measurements of the RAD7 are based on electrostatic collection of alpha-emitters with spectral
analysis. Measuring with the “Normal” mode counts decays of both Polonium decay products of ²²²Rn
155 (218Po, 214Po). The counts were measured over one hour and averaged, with a standard deviation of one

sigma and expresses as decays per second [Bq]. The measurement range lies between 4 – 750000 Bq m⁻³ with an accuracy of ± 5 %.

The ²²²Rn concentration in 300 mL samples from ground water (2.3.3) and the river was measured with the Wat250 mode. In addition, soil ²²²Rn emissions were estimated with closed chamber measurements
160 with the RAD7 over 3h (one Rn measurement per hour). Assuming that groundwater is the main source of CO₂ and that ²²²Rn moves at the same mass flow as CO₂ (Megonigal et al. 2020), the same spatial dependence of CO₂ and ²²²Rn fluxes would be expected in case of groundwater being the major source of CO₂. For this reason, ²²²Rn chamber measurements were performed simultaneously at two different positions, one with low and one with high CO₂ flux. We used two chambers of different size and corrected
165 ²²²Rn flux measurements [Bq m⁻³ d⁻¹] for different chamber geometry by multiplying with the volume [m³] and dividing by the area [m²] of the chamber to get the ²²²Rn flux [Bq m⁻² d⁻¹].

2.3.3 Water + sediment sampling

For groundwater sampling piezometers with a diameter of 2.7 cm and a length of 100 cm were installed next to each collar (Figure S1b) a day before the sampling campaign.

170 To determine the thickness of the unsaturated zone, the water level in the piezometers was measured with an electric contact gauge. *In situ* parameters pH, conductivity, temperature, and O₂ saturation were measured in the piezometers and the river with a multiparameter probe (WTW® MultiLine® Multi 3630 IDS, Xylem, Rye Brook, New York, USA). To analyze dissolved CO₂ and CH₄ concentrations, water samples were taken from the piezometers and the river using a syringe. Atmospheric air was added, with
175 a headspace ratio of 1:1. After shaking for 2 minutes the headspace was transferred to 12 ml evacuated Exetainers (Labco Exetainers®, Labco Limited, Lampeter, UK) and stored till further analysis in the laboratory. Air samples were taken for headspace correction. Water samples for chemical analysis were collected in crimp vials without a headspace, stored at 4 °C and later analyzed in the laboratory.

Soil samples from the 0-5 cm layer were taken around each collar for incubation experiments. Samples
180 were filled into plastic bags, stored at 4°C, and were analysed in the laboratory within a week.

2.3.4 Potential CO₂ production in laboratory incubations of sediment

Incubation experiments were set up to analyze the potential microbial respiration in dry river sediments under controlled conditions. For this purpose, fresh soil samples (25 g wet weight), taken along the transect were incubated in ~ 130 ml vials in replicates of four at 19.5 °C. To determine the temperature dependence of microbial respiration, 4 replicate samples of 25 g were incubated at 4, 12, 19.5, 28 and 35 °C. From each vial, 4 to 5 gas samples were taken over an incubation period of 2 to 3 days by a Pressure-Lok® syringe (Pressure-Lok® glass syringe, Valco Instruments, Waterbury, Houston, USA) and analyzed by gas chromatography for CO₂. Respiration rates were calculated from the linear increase of the CO₂ content in the incubation vials divided by dry sediment weight.

To evaluate the temperature response of the microbial respiration in the sediment the Q₁₀ temperature coefficient and the activation energy (E_a) was calculated (Dell et al. 2011). The activation energy was calculated as the slope of Arrhenius plots as described in Gillooly et al. (2001).

To compare respiration data from lab incubations to CO₂ fluxes measured in the field rates rates of respiration per gram dry weight [$\mu\text{mol g-dw d}^{-1}$] were converted to fluxes by multiplying with sediment bulk density [g-dw cm^{-3}] and the thickness of the reactive sediment layer which we assume to be equal to the thickness of the unsaturated zone [cm].

2.4 Analytics

CO₂ and CH₄ concentrations in gas samples were measured with a gas chromatograph (GC) (SRI 8610C, SRI Instruments Europe, Bad Honnef, Germany). The GC was equipped with a flame ionization detector and a methanizer which allowed simultaneous measurement of CO₂ and CH₄ with an accuracy of < 5 %. Dissolved gas concentrations were calculated using temperature dependent Henry coefficients (UNESCO/IHA 2010). Because the carbonate system in the headspace vial may change during headspace equilibration CO₂ concentrations were corrected for alkalinity as described in Koschorreck et al. (2021). To analyze dissolved inorganic carbon (DIC) and dissolved organic carbon (DOC) water samples were filtered with a glass microfiber filter (Whatman GF/F). DIC and DOC concentrations were analyzed based on high-temperature oxidation and NDIR-Detection (DIMATOC® 2000, DIMATEC Analysentechnik, Essen, Germany). The alkalinity of the water samples was determined by titration with HCl to pH of 4.3.

To determine the concentration of the cations K^+ , Na^+ , Ca^{2+} and Mg^{2+} the water samples were filtered with a 0.45 μm syringe filter, acidified with HNO_3 and analyzed with an ICP OES (Optima 7300 DV, Perkin Elmer, USA). The Anion concentrations of SO_4^{2-} and Cl^- were measured with ion chromatography (Dionex-ICS 6000, Thermo Fisher Scientific, Waltham, Massachusetts, USA).

Soil samples were analyzed to determine soil moisture content, bulk density, and organic matter from weight loss after drying for at least 2 days to constant weight at 105 °C and loss on ignition (LOI) at 550°C, respectively. Sediment texture was determined by the FAO method (FAO 2020).

2.5 Statistics

CO_2 flux data sets from manual and automatic measurements were visually checked for normality distribution with Q-Q-plots. Data were summarized by distance to the river and tested with a one-sample t-test to determine if measured fluxes differed significantly from zero.

Spearman rank correlation was used to identify relationships between environmental variables and the observed CO_2 flux, and to identify the strength and direction of these relations (Leyer and Wesche 2007). Additionally, representative periods and single days were selected from automatic measurements to analyze patterns, hidden by the temporal variability of the data. The measured environmental variables of sediment temperature, sediment moisture, thickness of the unsaturated zone, organic matter content, and precipitation were used for correlation analysis. Water level and climate data were averaged over 1 hour.

Linear mixed-effects models (lme) were applied to predict the influence of the environmental variables on the CO_2 flux at the study site for variables for which a linear relationship with the CO_2 flux was presumed. Model selection was done by removing predictors and comparing conditional R^2 values of different models. To apply simple linear regression models and lme, assumptions of normality and homoscedasticity were visually checked with diagnostic plots, including residuals vs. fitted and Q-Q-plot.

Flux data were log transformed for lme analysis. Because of occasional small negative fluxes we shifted all fluxes to positive values by adding 121 $mmol\ m^{-2}\ d^{-1}$ prior to transformation (120 was the value of the largest negative flux). Statistical analysis was performed using R (R-Core-Team 2016).

3 Results

3.1 Long term data

235 The river showed a typical summer discharge situation with a water level mostly below 1 m, interrupted
by a high discharge event at the end of June (Figure 1). Considerable areas of dry sediments only emerged
during 6 weeks in early summer, and short periods in the first week of August and in September. CO₂
fluxes measured during these periods showed high diurnal and seasonal fluctuations (Figure 2). Fluxes
fluctuated over 3 orders of magnitude between -120 and 1135 mmol m⁻² d⁻¹ with a median of 98 and a
240 mean±SD of 149±155 mmol m⁻² d⁻¹. Fluxes fluctuated in a narrow range below 200 mmol m⁻² d⁻¹ during
the first phase of the investigations in May. Due to rising water level at May 17th we moved the chambers
higher up where we measured both higher fluxes and larger diurnal amplitudes. When the water level
decreased after May 20th we moved the chamber down to freshly emerged sediment. There, CO₂ fluxes
were similar to the fluxes measured 10 cm higher during the first half of May and tended to increase with
245 increasing time since drying. Negative fluxes were observed in 193 out of 3128 flux measurements (=6%
of all fluxes). Negative fluxes were observed especially during the beginning of the measurement period
and at sites near to the water. Interestingly, negative fluxes nearly exclusively occurred during the day
between 10:00 and 18:00, peaking in the afternoon (Figure S2). Chambers installed closer to the water
measured lower and less variable fluxes than chambers installed higher upslope.

250 Fluxes showed considerable short-term variability. Variability was not constant during the investigated
period but especially high after June. Clear diurnal patterns were observed during the entire study but
most pronounced in September.

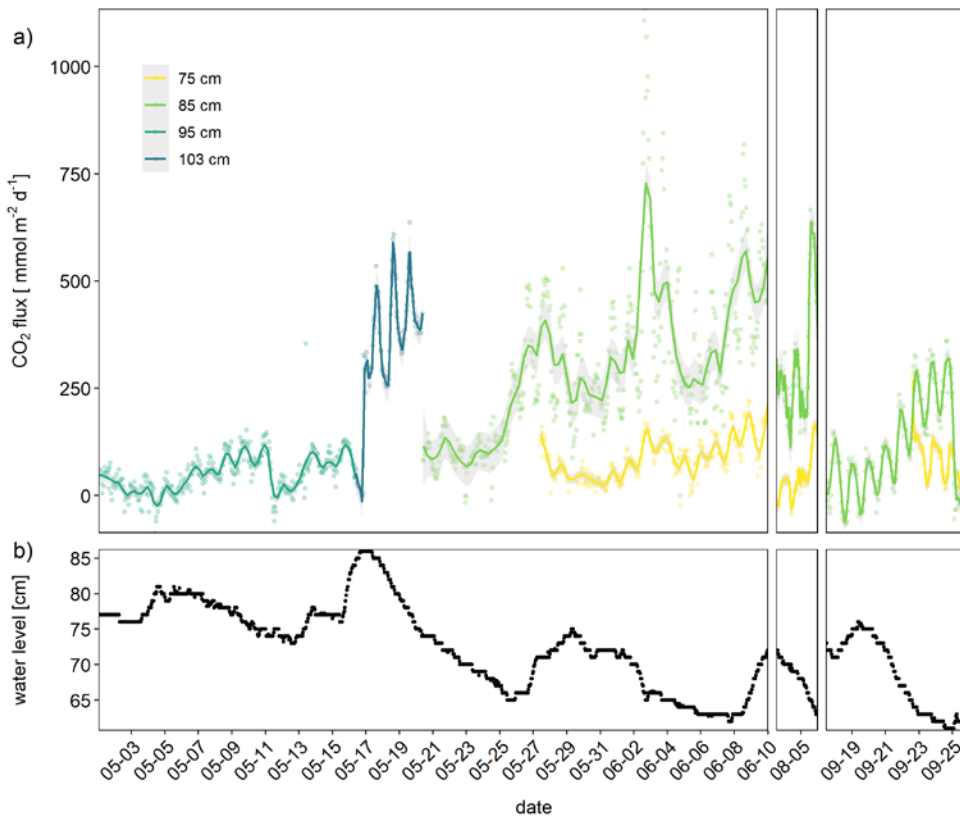


Figure 2: CO₂ fluxes in mmol m⁻² d⁻¹ measured with automatic chambers (a) and corresponding water level of the river measured 13 km downstream at the gauge “Magdeburg Strombrücke” (b). Colors indicate the elevation of the chambers. For example the “75 cm position” means that the chamber was directly above the water line when the gauge reading was 75. Lines indicate smoothed data ± SD using LOESS smoother with span 0.1. The grey areas indicate confidence intervals.

255

260 3.1.1 Regulatory factors: sediment moisture, temperature, water level, climate

The observed diurnal pattern with higher CO₂ fluxes during the day suggested a temperature regulation of the flux. The CO₂ flux was indeed weakly (spearman $p < 0.05$) correlated with the thickness of the

unsaturated zone ($R^2=0.31$), sediment temperature ($R^2=0.19$, Figure 3a) and moisture ($R^2=-0.19$), as well as precipitation ($R^2=-0.12$). A mixed effect linear model with site were the chamber was placed as random factor and temperature and thickness of the unsaturated zone as fixed factors explained 0.61 % of the variability. Adding moisture did not further improve the lme (Table S1).

The temperature response of the CO₂ flux was not very clear, however, if all data were plotted together (Figure 3a) but if data from single days were plotted a clear pattern emerged (Figure 3b and Figure S3). The temperature response of the flux was affected by the time of day resulting in typical hysteresis curves.

Warming during the day resulted in exponentially increasing fluxes. However, fluxes stayed high despite cooling started in the afternoon – the temperature response of the flux was clearly delayed. From the CO₂ flux-temperature relation (Figure 3a) an activation energy of 0.56 eV (37 kJ mol⁻¹) could be calculated which corresponds to a Q₁₀ of 1.7 between 10 and 20°C.

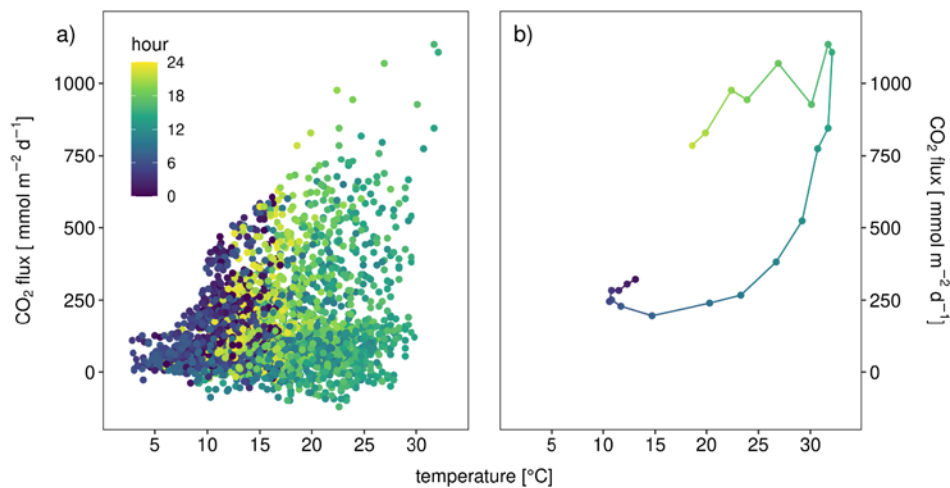


Figure 3: CO₂ flux in mmol m⁻² d⁻¹ (obtained from 3 automatic chambers) depending on sediment temperature (a) all data (b) only data from June 2nd as an example for hysteretic response to temperature. Color indicate hour of measurement.

A closer look at data from one week in September revealed how temperature, thickness of the unsaturated zone, and precipitation interacted in regulating the flux (Figure 4). Temperature drove the very clear diurnal amplitude but the absolute level of the flux was higher with increasing thickness of the unsaturated

280 zone (which was accompanied by sediment drying). A single precipitation event at September 25th resulted in a sudden increase in sediment moisture which was accompanied by a clear drop of the CO₂ flux. If only data for the period shown in Figure 4 were considered a linear model containing sediment temperature and moisture and the interaction between temperature and moisture explained 46 % of the variance.

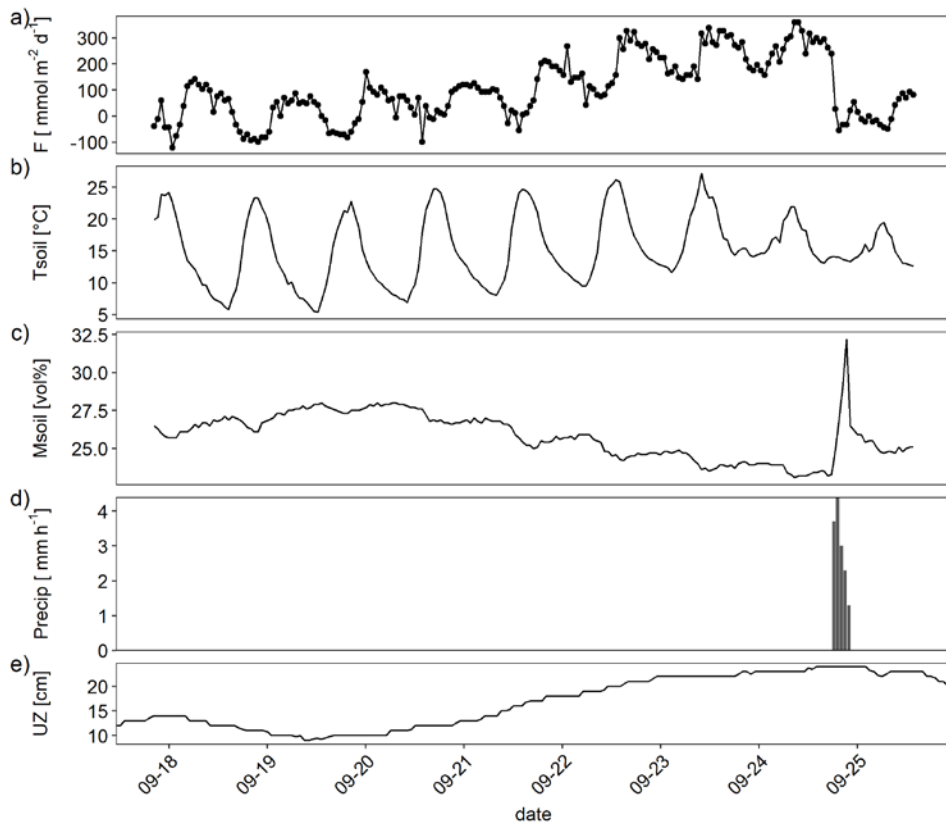


Figure 4: Example high frequency dataset showing (a) CO₂ flux (F) measured by an automatic chambers (b) sediment temperature (Tsoil; 0-5 cm depth) (c) sediment moisture (Msoil; 0-5 cm depth) (d) precipitation (Precip) recorded in hourly resolution and (e) thickness of the unsaturated zone (UZ; distance between water table level and ground surface).

3.1.2 Spatial gradient of CO₂ flux

290 Manual chamber measurements at different distance to the water revealed a spatial gradient of the CO₂ flux. CO₂ fluxes were lowest near to the water line where sediment moisture was highest (Figure 5) and fluxes increased with distance to the water. This was also visible in the automatic chamber data when chambers were placed at different distance to the water (compare Figure 2). The chamber which was placed nearer to the water recorded consistently lower fluxes. This is also consistent with the observed
295 positive correlation between CO₂ flux and the thickness of the unsaturated zone.

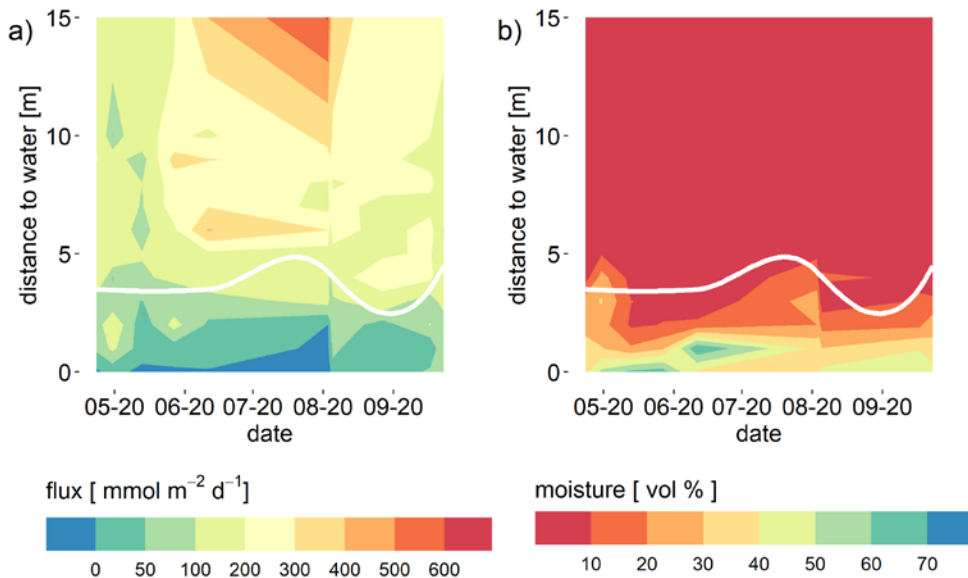


Figure 5: CO₂ flux (mmol m⁻² d⁻¹) as measured with a manual chamber (a) and sediment moisture (vol-%) measured with a probe in 0-5 cm depth (b) depending on the distance to the water. The white lines indicates the "plant line". The areas below this line was free of vegetation (never plants inside chambers).

300 We also observed higher CO₂ fluxes in the vicinity of plants. Plants were consistently found from about 3 m from the water uphill. Fluxes above this "plant line" (indicated by the white line in Figure 5) tended to be higher than fluxes from the vegetation free area nearer to the water.

In sum, our field based measurements provide strong evidence that respiration in the sediment was the major driver of the observed CO₂ flux. To further support this conclusion detailed investigations were carried out.

3.2 Detailed investigations

The sediment pore water was quite similar to river water with respect to electric conductivity and dissolved solutes including DIC (Table 1). The water level difference between the wells and the river was below the detection limit – the hydraulic gradient was virtually zero during our sampling campaigns. The shallow hydraulic gradient and the similar chemistry suggest a large influence of river water on the sediment pore water. In contrast, concentrations of dissolved gases were quite different with high concentrations of CO₂ and CH₄, and low concentrations of O₂ in the pore water. Pore water concentrations of CO₂ increased with distance to the river while CH₄ concentrations tended to be highest near the river. In August the river water was slightly under saturated with respect to CO₂. The sediment was poor in organic matter (LOI < 1%) and texture was loamy sand. GHG emissions were dominated by CO₂ while CH₄ fluxes were low and N₂O fluxes always below the detection limit (Table 1).

Table 1: Sediment, groundwater, and river water properties at the 2 sampling campaigns

parameter	unit	August 4 th 2020				September 23 th 2020					
distance to river	m	river	1	3	5	6	river	1	2	3	4
CO ₂ flux	mmol m ⁻² d ⁻¹	-3	33	87	153	153	36	103	49	142	126
CH ₄ flux	mmol m ⁻² d ⁻¹	0.7	3.4	0	0	0.6	6	0.5	0	0	-0.6
unsaturated zone	cm	10	31	62	78		9	19	32	36.5	
moisture	[vol %]		30	13	25	12		30	25	-	9
organic matter in sediment	[% LOI]		0.78	0.39	1.11	0.94		0.85	0.97	-	0.52
CH ₄	μmol L ⁻¹	0.3	18	11	11	6	2.5	189	186	212	70

CO ₂	μmol L ⁻¹	13.3	610	883	1960	3681	32	1193	899	1118	1024
DIC	mg L ⁻¹	42	23	48	49	50	24	70	64	64	55
alkalinity	mg L ⁻¹	1.9	3.5	3.5	3.6	3.1	1.9	4.5	4.8	5.3	4.7
DOC	mg L ⁻¹	13.1	6.9	9.3	12	13.5	6.31	9.4	9.9	11.5	11
SO ₄ ²⁻	mg L ⁻¹	79	44	71	67	74	79	7.3	20	31	92
pH		8.3	7.2	6.8	6.6	6.6	8	7.2	7.3	7.2	7
conductivity	μS cm ⁻¹	640	610	658	640	1563	601	696	655	647	640
O ₂	mg L ⁻¹	9.1	0.8	1.1	1.9	2	9.3	3.4	2.5	4	4

Diffusive fluxes from the river were calculated from concentrations using the gas transfer coefficient from Matoušů et al. (2019).

320 3.2.1 CO₂ fluxes versus Rn fluxes

Groundwater contained more than one order of magnitude higher Rn concentrations than the river water (Table 2). As an indicator of groundwater degassing and possible evasion of CO₂, we measured the flux of radon out of the sediment, assuming groundwater as a major source. Rn fluxes were higher in September than in August although the Rn concentration in the groundwater was similar in both months
325 (Table 2). The flux of radon out of the sediment was, however, not much different at two different distances to the river while the CO₂ flux differed by about one order of magnitude between the same sites. If groundwater was the source of CO₂, we would expect Rn fluxes to be related to CO₂ evasion from groundwater; thus our data indicates that higher CO₂ fluxes were not originating from groundwater.

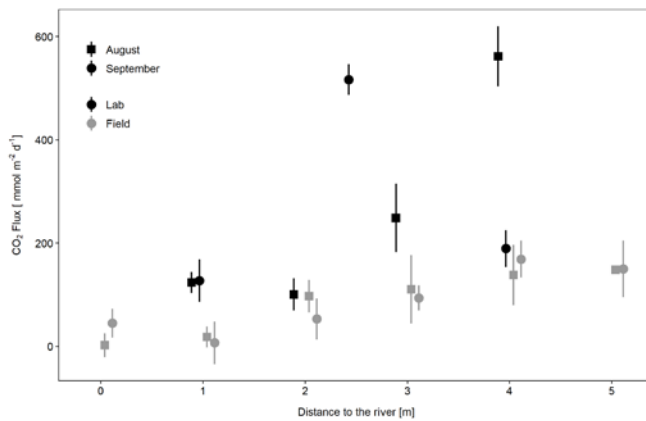
330 **Table 2: Flux of radon measured as ²²²Rn increase in static chambers compared to CO₂ flux measured in the same chambers, and radon concentration determined as detected activity (Bq m⁻³) in the groundwater sampled in wells directly beside the chambers as well as in the river water (0 m distance).**

date	Distance to river [m]	²²² Rn flux [Bq m ⁻² d ⁻¹]	CO ₂ flux [mmol m ⁻² d ⁻¹]	²²² Rn in water [Bq m ⁻³]
	0			327±109
08-05	1	65	18±20	6090±418
	3	63	110±31	
09-23	0			532±135

1	174	7±41	6650±436
4	205	169±36	

3.2.2 Sediment respiration rates

To check whether the observed CO₂ fluxes could be explained by microbial respiration in the sediment, laboratory incubations were carried out. Sediment respiration rates as measured in laboratory incubations were 0.9±0.45 μmol g⁻¹ d⁻¹ in August and 0.64 μmol g⁻¹ d⁻¹ in September with rates increasing with distance to the river. Potential CO₂ fluxes calculated from these rates were similar or higher than CO₂ fluxes measured *in situ* (Figure 6). Thus, sediment respiration was high enough to explain the observed CO₂ emissions.



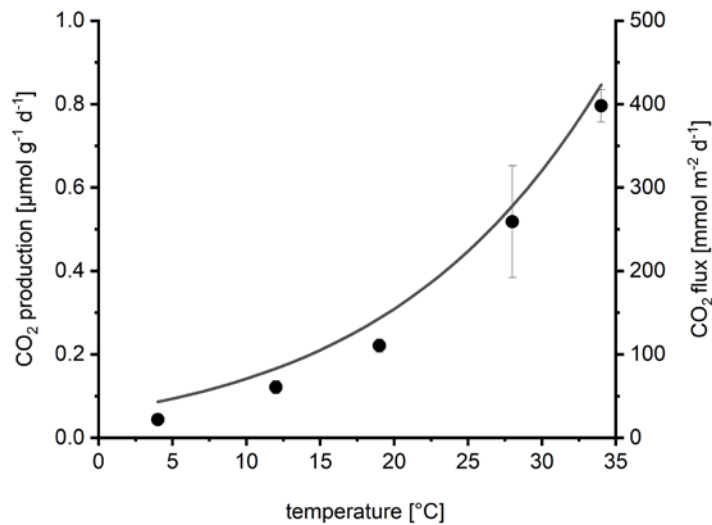
340 Figure 6: Potential CO₂ flux determined from laboratory incubations of sediment compared to *in situ* CO₂ fluxes depending on distance to the river. Potential fluxes per unit area were calculated from sediment respiration rates (mmol g⁻¹ dw d⁻¹), the thickness of the unsaturated zone (cm), and the bulk density of the sediment (g dw cm⁻³).

3.2.3 Temperature dependence of sediment respiration

Sediment respiration increased exponentially with temperature (Figure 7) resulting in a Q₁₀ of 2.5. The calculated activation energy of 0.7 eV was similar to the activation energy calculated from the automatic chamber data. The comparison with the temperature response of the CO₂ flux measured by the automatic

345

chambers (line in Figure 7) visualizes the similar temperature response of sediment respiration and *in situ* fluxes.



350 Figure 7: Temperature dependence of Sediment CO₂ production (=sediment respiration) in laboratory incubations depending on temperature (dots show mean \pm SD of 4 replicates). For comparison, the line shows the average temperature response of the CO₂ flux measured by automatic chambers, calculated by fitting the data from Figure 3a to the Arrhenius equation.

4 Discussion

4.1 Source of the CO₂

355 Both our continuous data and detailed measurements show that the CO₂ emitted from dry Elbe sediments originated from respiration in the sediment rather than from groundwater. This conclusion is consistently supported by numerous evidence:

- The observed CO₂ fluxes could be fully explained by sediment respiration measured in laboratory incubations. From soil respiration measurements it is well known that basal respiration as measured in laboratory incubations cannot be equaled with soil CO₂ emissions (Reichstein et al.

360

2000). A major difference between both methods is the exclusion of root respiration in bottle incubations which would lead to an under estimation of total soil respiration in root free assays such as bottle incubations (Hanson et al. 2000). Thus, our sediment respiration rates measured in the laboratory are probably conservative estimates which even strengthens our argumentation.

- 365 • The temperature response of the CO₂ flux was very similar to the measured temperature response of sediment respiration and showed Q₁₀ values typical for biological processes (Yvon-Durocher et al. 2012) and soil respiration (Hamdi et al. 2013). Potential evaporation on the other hand depends on radiation, vapor pressure, and wind speed (Penman 1948) and only indirectly on surface temperature (Kidron and Kronenfeld 2016). The temperature dependence of evaporation of soils depends on a complex interaction of texture and soil moisture, and is not easy to predict (e.g. (Federer 2002)). The observed temperature dependence provides strong evidence for respiration being the primary driver of the CO₂ flux.
- 370 • CO₂ emissions increased with distance to the river. If groundwater was a major source of CO₂ emissions we would expect higher emissions at lower sediment elevation were groundwater potentially exfiltrates into the sediment. If there was a hydraulic groundwater gradient towards the river this gradient should be steepest near to the river resulting in highest groundwater flux and potential outgassing near the river.
- 375 • The CO₂ flux was proportional to the volume of the unsaturated sediment. If CO₂ originated from groundwater emissions we would expect even a negative correlation because the transport of CO₂ from the groundwater surface to the sediment surface should be inhibited by a larger unsaturated zone.
- 380 • Higher CO₂ emissions were not accompanied by higher Rn emissions. Groundwater typically contains high Rn concentrations and Rn is a proven tracer to investigate groundwater input into surface waters (Cook and Herczeg 2000; Perkins et al. 2015). We observed emission of Rn from the sediments indicating some influence of groundwater on the sediments. Rn emission at different distance from the river were identical. Thus, the thickness of the unsaturated sediment did not affect Rn emissions, showing that the anoxic zone itself was probably not a source of Rn. Soil Rn concentrations are known to be affected by meteorological and soil physical conditions (Asher-
- 385

390 Bolinder et al. 1971). Similar Rn emissions, as observed in our study, are therefore an indication
for similar sediment physical conditions. However, the magnitude of Rn emissions did not
correspond to the magnitude of the CO₂ emissions, indicating that the CO₂ flux was independent
from groundwater outgassing.

- As we did not see hydraulic gradients indicative of larger groundwater inflow at our location of
study, CO₂ concentrations in the groundwater were too low to explain the observed CO₂ flux.
395 Groundwater degassing is relevant in situation when groundwater is pumped to the surface (Wood
and Hyndman 2017) or seeps into surface waters (Duvert et al. 2018). In rivers it might be relevant
at seep sites which probably especially occur after fast water level drops and at extremely low
water level.

Taken together our data consistently show that the observed CO₂ emissions originated from respiratory
400 CO₂ production in the sediment. After having identified the primary source of CO₂ we now look on the
regulators of the magnitude of the CO₂ emissions.

4.2 Regulation of CO₂ emissions

Temperature is a master variable regulating several biogeochemical processes. Our temperature
dependence ($Q_{10} = 2.5$, E_a 0.7 eV) is in line with the temperature response of numerous ecological
405 processes. A meta analysis of 63 studies of temperature dependence of soil respiration revealed a mean
 Q_{10} of 2.6 (Hamdi et al. 2013). Diverse types of ecosystems have an activation energy of respiration of
0.65 eV (Yvon-Durocher et al. 2012) which is very similar to our study.

Temperature was an important regulator not only because of the temperature dependence of sediment
respiration but also because the diurnal temperature amplitude was quite large. Sediment temperature not
410 only ranged between 2.8 and 32°C during the study period but the complete temperature amplitude of
about 20°C could be observed during single days (Figure 4). The large diurnal amplitude at these sites is
favored by a lack of shadow and the fast heating of the sand which can lead to temperatures easily
exceeding 40°C (Mallast et al. 2020).

Although the temperature dependence of the CO₂ flux is evident, it was not easily visible in flux versus
415 temperature plots which show a large scatter (Figure 3a). Only when looking at single days a typical

hysteresis pattern (Figure 3b) became apparent. Such hysteresis curves have frequently been observed in high frequency datasets of soil respiration (e.g. (Riveros-Iregui et al. 2007)). They originate from a phase lag between temperature and CO₂ flux and can be explained by different transport of heat and CO₂ in soils (Phillips et al. 2011) or by variable C supply from plants (Oikawa et al. 2014). The rotation direction as well as the shape of the ellipsoid depends on the vertical profile of temperature and activity in the soils as well as on the depth where soil temperature was measured. We measured temperature in 5 cm depth and obtained anticlockwise hysteresis which means that CO₂ emissions were delayed relative to temperature measurements. A plausible explanation is that a large part of the CO₂ was produced in deeper sediment layers where the daily temperature maximum was reached later. This is consistent with the observed positive correlation between CO₂ flux and the thickness of the unsaturated zone. Theoretically the effect could also be caused by delayed outgassing of CO₂ from deeper sediment layers due to CO₂ transport limitation. However model calculations had shown that this mechanism was less relevant for shaping diurnal hysteresis in soils (Phillips et al. 2011). We quantified the delay by shifting flux and sediment-temperature data against each other (Figure 8). By correlating the flux with the temperature 3 hours before we obtained the best linear correlation ($R^2=0.97$) for the data in Figure 3b. However, the time shift which produced the best linear fit differed between days (min=0, max=10, mean \pm SD = 4.8 \pm 3.7 h) with a median of 4 hours and no apparent differences between sites. Also the R^2 of the best fit differed between 0.2 and 0.97. Thus, the hysteresis pattern obviously depended on the day of measurement and it is not possible to derive a general relation which then could be used to analyze temperature-flux relations of time-shift corrected data.

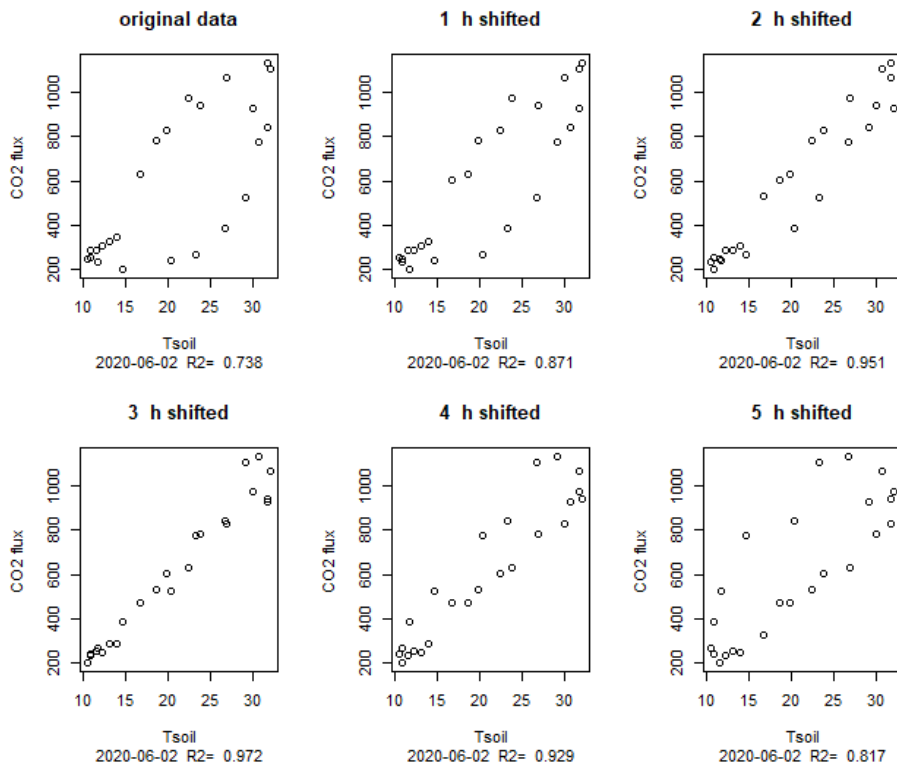


Figure 8: Hysteresis loop for June 2nd (same data as in Figure 3b) with flux data shifted for various hours. 3 hours shifted means that the flux at 10:00 was correlated with the temperature at 7:00.

440 Wetting of dry soils typically triggers a pulse of CO₂ production (Birch 1958). However, in our case
 441 wetting events caused by rainfall reduced the CO₂ flux as exemplified in Figure 4. This shows that CO₂
 442 production in the sediment was not water limited and/or that the CO₂ flux was rather transport limited
 443 when rain water blocked gas filled pores (Asher-Bolinder et al. 1971). At sediment moisture around 30%
 444 in sandy sediments as measured in our study microbial activity in the sediment is probably not water
 445 stressed and consequently not stimulated by wetting. Thus, it is probable that the reduced CO₂ flux after

rain events was caused by physical blocking of soil pores. This is consistent with the observed long term increase of the CO₂ flux with decreasing moisture. Direct mechanistic dependence, however, is difficult to show because moisture also correlates with the thickness of the unsaturated zone (=water level of the river relative to the sediment surface). This is why adding moisture to our mixed model only marginally
450 increased the predictive power of the statistical model.

The thickness of the unsaturated zone was a strong predictor of the CO₂ flux. The entire unsaturated zone obviously contributed to the CO₂ flux. This is plausible because the intermediate sediment moisture both favored microbial processes and enabled gas exchange through gas filled pores. This may also explain high CO₂ fluxes in situations with extremely high sediment surface temperature (Mallast et al. 2020).
455 Even if under such conditions CO₂ production is inhibited at the surface respiration in deeper layers may maintain high CO₂ emissions.

The occurrence of vegetation, although excluded from our chamber measurements and restricted to the vicinity of the chambers, obviously is a game-changer, largely stimulating sediment CO₂ emissions. From our data we cannot fully distinguish whether higher fluxes near plants were caused by the plants or only
460 by distance to the water (which is equivalent to the thickness of the unsaturated zone). However, the thickness of the unsaturated zone increased continuously while the “plant line” represents a sudden change of conditions. Our data show a consistent high CO₂ flux above the “plant line”. It is well known that root respiration may contribute about 50% to soil respiration (Hanson et al. 2000) and soil respiration is typically correlated with root biomass (Tufekcioglu et al. 2001). Thus, as we did not use trenched collars
465 to exclude roots from chamber fluxes, it is highly probable that plants contributed to the elevated CO₂ emissions through root respiration or provision of root exudates above the “plant line”. Higher sediment CO₂ emissions, however, do not mean net CO₂ emissions from the ecosystem since the vegetation growing on the dry sediments also fixes carbon and can even turn exposed sediments into a carbon sink (Bolpagni et al. 2017). To assess the effect of emerging vegetation on the overall carbon cycle of dry
470 sediments other methods like plant biomass determination or flux measurements including photosynthesis in transparent chambers are necessary.

4.3 CO₂ uptake by the sediment

We frequently observed CO₂ uptake by the sediment, although there were no plants and no light in our chamber. This is known from other studies and has been attributed to inorganic processes (Ma et al. 2013; 475 Marcé et al. 2019). In our case the observed CO₂ uptake could also be explained by the interaction of the sediment with river water. During May and June the river was under saturated with CO₂ (Figure S4). The groundwater chemistry data show a gradient of concentrations increasing with distance to the river. This shows that the sediment pore water near to the river was affected by river water. Interestingly, negative fluxes were nearly exclusively observed during the daylight hours. A plausible explanation would be that 480 ship induced wave action might have triggered occasional river water intrusion and CO₂ uptake by the sediment (Hofmann et al. 2010). This mechanism, however, cannot explain negative fluxes in September when the river was over saturated with CO₂ (Figure S4).

Dark CO₂ uptake could theoretically be caused by chemoautotrophic micro-organisms like nitrifiers. However, chemoautotrophic CO₂ uptake should not be stimulated by light and is thus not consistent with 485 our observation of nearly exclusive CO₂ uptake during the day.

A straightforward explanation for negative CO₂ fluxes during the day is CO₂ uptake by phototrophic organisms. Algae and cyanobacteria are well known to have active carbon concentrating mechanisms (CCM) which allow CO₂ uptake also in the dark (Giordano et al. 2005). Phototrophs living at the surface of dry sediments are facing a harsh environment with high salinity in thin water films covering particles and high irradiation and temperature – all factors favoring the activation of CCMs (Beardall and Giordano 490 2002). Dark CO₂ uptake is a common observation in ¹⁴CO₂ uptake measurements and known to depend on pre-darkness light conditions (Legendre et al. 1983). In pure cultures it has been shown that CO₂ uptake by algae may proceed for more than an hour in darkness (Goldman and Dennett 1986; Ohmori et al. 1984). Thus, it is highly plausible that the observed CO₂ uptake by dry sediments was caused by 495 photosynthetic algae and/or cyanobacteria. Future studies including chlorophyll analysis of sediments or the application of specific inhibitors may clarify the mechanism behind CO₂ uptake in exposed river sediments.

4.4 Implications

500 Photosynthetic uptake of CO₂ in the dark would have consequences for the interpretation of dark chamber measurements. If a chamber is placed on the sediment photosynthetic CO₂ uptake may proceed for an unknown period of time. The fact that no net uptake was observed in the night shows that the capability of dark CO₂ uptake could not be sustained for periods longer than one hour, which is consistent with pure culture observations (Goldman and Dennett 1986). However, flux measurements are usually performed within a few minutes making it highly probable that they include eventual photosynthetic CO₂ uptake.

505 Comparison of transparent and opaque chamber measurements are sometimes used to detect photosynthesis of algae. Our results imply that such interpretation have to be treated with care because photosynthetic CO₂ uptake may proceed during dark flux measurements.

Our median CO₂ flux of 98 mmol m⁻² d⁻¹ would result in annual emissions of 429 g C m⁻² y⁻¹ which is in the range of fluxes typical for temperate ecosystems (Doering et al. 2011) and similar to fluxes reported 510 for dry Elbe sediments (Mallast et al. 2020), but high compared to the gravel bed of an alpine river (38 mmol m⁻² d⁻¹, (Doering et al. 2011)), and low compared to exposed sediments of Mediterranean streams (781 mmol m⁻² d⁻¹, Gómez-Gener et al. (2016)). Although our observations thus fit the reported range, these differences as well as the large variation of fluxes observed in our high frequency measurements (-120 to 1135 mmol m⁻² d⁻¹ – this range is larger than the range of typical fluxes for all kinds of terrestrial 515 ecosystems as compiled by (Doering et al. 2011)) implies that care must be taken when upscaling fluxes for certain ecosystems but also for larger scales.

The observed hysteresis obscures flux-temperature relations if measurements were only performed at one time during the day. Thus, temperature regulation of dry sediment CO₂ emissions might be more relevant and more complex than identified in a recent study (Keller et al. 2020).

520 Our high frequency measurements show that standard measuring protocols are probably under estimating CO₂ emissions from dry sediments because high fluxes in the night resulting from a delayed temperature response are not considered. The median flux measured between normal working hours (8:00 – 18:00) was 87 mmol m⁻² d⁻¹ compared to 98 mmol m⁻² d⁻¹ if all data were considered. Thus, only measuring during daytime would lead to a flux under estimation of 11%. We therefore recommend to assess temporal

525 shifts in flux-temperature responses in order to obtain better estimates for upscaling based on a
representative choice of flux data.

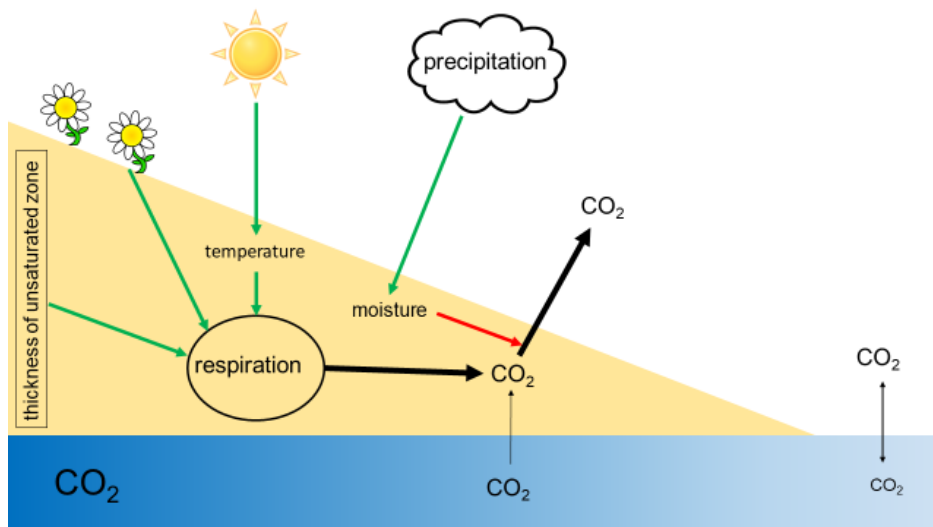
Our results are partly contradicting results from (Mallast et al. 2020) who observed highest CO₂ emissions
near to the waterline. The two studies, however, are not directly comparable because the previous study
by (Mallast et al. 2020) was carried out under extreme drought conditions. Under such conditions deeper
530 lying sediments which tend to be higher in organic matter and less sandy were exposed to the atmosphere.
Such conditions should favor CO₂ emissions (Keller et al. 2020). Furthermore the very dry conditions
(<10% sediment moisture) under the extreme drought might have inhibited microbial processes in the
sandy sediment. While the drivers of CO₂ emissions from dry sediments are known, their complex
interaction makes it difficult to predict CO₂ emissions under a given situation.

535 The observed relation between CO₂ flux and distance to the river, however, might facilitate upscaling of
CO₂ emissions from dry river sediments. The width of the dry sediment zone can be extracted from
satellite images or aerial photographs. The observed consistent spatial pattern also implies that the CO₂
flux was probably not much affected by time after exposure. Thus, combining few diurnal datasets of CO₂
flux and lateral transects with seasonal data of the width of the dry sediments zone along a river is a
540 promising approach to quantify total CO₂ emissions from such systems.

5 Conclusions

We could clearly show that CO₂ emissions from dry river sediments under the given conditions here were
primarily driven by respiration in the sediment. Thus, existing knowledge about soil respiration might
also apply to dry river sediments.

545 We could further show that CO₂ emissions were regulated by temperature and the thickness of the
unsaturated zone (Figure 8). The observed hysteresis effect clearly show that simple correlations between
environmental parameters and CO₂ emissions from sediments may be too simplistic to study regulatory
mechanisms. Positively spoken the analysis of such hysteresis relations may allow conclusions about
underlying mechanisms (Musolff et al. 2021).



550

Figure 9: Scheme of processes and drivers of CO₂ fluxes from dry river sediments. Green arrows indicate positive, red arrows negative effects.

Our data show that the occurrence of terrestrial vegetation has a large and not yet assessed impact on the carbon cycle of dry sediments. To assess the effect of vegetation not only ecosystem production has to be quantified but also the fate of plant biomass upon re-flooding. While it is clear that CO₂ emissions from dry river sediments are relevant the exact quantification of the effect of low river levels on the river carbon cycle remains challenging. Short term temporal variation is very high and probably equally relevant as seasonal variability. Any attempt to quantify annual GHG emissions or the relevance of dry river sediments for carbon cycling needs to address temporal dynamics of CO₂ emissions from dry river sediments.

560

6 Data availability

The high frequency dataset is supplied as a supplement.

7 Supplement link

8 Author contribution:

565 MK initiated the study and prepared the manuscript with contributions from all co-authors. LT and MK performed measurements. All authors planned measurements and discussed the results.

9 Competing interests

The authors declare that they have no conflict of interest.

10 Acknowledgements

570 Thanks to Martin Wieprecht for his excellent help during fieldwork and to Ulrike Berning-Mader and Corinna Völkner for their instructions and help in the laboratory of the Westfälische Wilhelms-University and UFZ. Thanks to Prof. Christian Wilhelm for advice regarding dark CO₂ fixation, Bertram Boehrer for discussion and to Peifang Leng for help using R. This work was supported by funding from the Helmholtz Association in the framework of Modular Observation Solutions for Earth Systems (MOSES).

575 11 References

- Asher-Bolinder, S., D. E. Owen, and R. R. Schumann. 1971. A PRELIMINARY EVALUATION OF ENVIRONMENTAL FACTORS INFLUENCING DAY-TO-DAY AND SEASONAL SOIL-GAS RADON CONCENTRATIONS. *In* L. C. S. Gundersen and R. B. Wanty [eds.], Field Studies of radon in rocks, soils, and water. U.S: Geological Survey.
- 580 Battin, T. J., S. Luysaert, L. A. Kaplan, A. K. Aufdenkampe, A. Richter, and L. J. Tranvik. 2009. The boundless carbon cycle. *Nature Geoscience* **2**: 598-600.
- Beardall, J., and M. Giordano. 2002. Ecological implications of microalgal and cyanobacterial CO₂ concentrating mechanisms, and their regulation. *Funct. Plant Biol.* **29**: 335-347.
- 585 Birch, H. F. 1958. The effect of soil drying on humus decomposition and nitrogen availability. *Plant Soil* **10**: 9-31.
- Bolpagni, R., S. Folegot, A. Laini, and M. Bartoli. 2017. Role of ephemeral vegetation of emerging river bottoms in modulating CO₂ exchanges across a temperate large lowland river stretch. *Aquat. Sci.* **79**: 149-158.

Formatiert: Englisch (USA)

- Bolpagni, R., A. Laini, T. Mutti, P. Viaroli, and M. Bartoli. 2019. Connectivity and habitat typology drive CO₂ and CH₄ fluxes across land–water interfaces in lowland rivers. *Ecohydrology* **12**: e2036.
- Bussmann, I., U. Koedel, C. Schütze, N. Kamjunke, and M. Koschorreck. 2022. Spatial Variability and Hotspots of Methane Concentrations in a Large Temperate River. *Front Env Sci-Switz* **10**.
- Cook, P. G., and A. L. Herczeg. 2000. *Environmental Tracers in Subsurface Hydrology*. Springer.
- Coppola, E., M. Verdecchia, F. Giorgi, V. Colaiuda, B. Tomassetti, and A. Lombardi. 2014. Changing hydrological conditions in the Po basin under global warming. *Sci Total Environ* **493**: 1183-1196.
- Dell, A. I., S. Pawar, and V. M. Savage. 2011. Systematic variation in the temperature dependence of physiological and ecological traits. *P Natl Acad Sci USA* **108**: 10591-10596.
- Doering, M., U. Uehlinger, T. Ackermann, M. Woodtli, and K. Tockner. 2011. Spatiotemporal heterogeneity of soil and sediment respiration in a river-floodplain mosaic (Tagliamento, NE Italy). *Freshwat. Biol.* **56**: 1297-1311.
- Duvert, C., D. E. Butman, A. Marx, O. Ribolzi, and L. B. Hutley. 2018. CO₂ evasion along streams driven by groundwater inputs and geomorphic controls. *Nature Geoscience* **11**: 813-818.
- DWD. 2020. Datenbasis. Einzelwerte gemittelt. In D. Wetterdienst [ed.]. *German Weather Service*.
- FAO. 2020. Soil testing methods: global soil doctors programme-a farmer to farmer training programme., Soil testing methods manual.
- Federer, C. A. 2002. BROOK 90: A simulation model for evaporation, soil water, and streamflow.
- Gillooly, J. F., J. H. Brown, G. B. West, V. M. Savage, and E. L. Charnov. 2001. Effects of size and temperature on metabolic rate. *Science* **293**: 2248-2251.
- Giordano, M., J. Beardall, and J. A. Raven. 2005. CO₂ concentrating mechanisms in algae: Mechanisms, environmental modulation, and evolution. *Annu. Rev. Plant Biol.* **56**: 99-131.
- Goldman, J. C., and M. R. Dennett. 1986. Dark CO₂ Uptake by the Diatom *Chaetoceros-Simples* in Response to Nitrogen Pulsing. *Mar. Biol.* **90**: 493-500.
- Gómez-Gener, L. and others 2016. When Water Vanishes: Magnitude and Regulation of Carbon Dioxide Emissions from Dry Temporary Streams. *Ecosystems* **19**: 710-723.
- Gomez-Gener, L. and others 2015. Hot spots for carbon emissions from Mediterranean fluvial networks during summer drought. *Biogeochemistry* **125**: 409-426.
- Hamdi, S., F. Moyano, S. Sall, M. Bernoux, and T. Chevallier. 2013. Synthesis analysis of the temperature sensitivity of soil respiration from laboratory studies in relation to incubation methods and soil conditions. *Soil Biology & Biochemistry* **58**: 115-126.
- Hanson, P. J., N. T. Edwards, C. T. Garten, and J. A. Andrews. 2000. Separating root and soil microbial contributions to soil respiration: A review of methods and observations. *Biogeochemistry* **48**: 115-146.
- Hofmann, H., L. Federwisch, and F. Peeters. 2010. Wave-induced release of methane: Littoral zones as a source of methane in lakes. *Limnol. Oceanogr.* **55**: 1990-2000.
- Keller, P. S. 2020. glimmr: Compute gasfluxes with R. *Gas Fluxes and Dynamic Chamber Measurements*.
- Keller, P. S. and others 2020. Global CO₂ emissions from dry inland waters share common drivers across ecosystems. *Nature Communications* **11**: art. 2126.
- Kidron, G. J., and R. Kronenfeld. 2016. Temperature rise severely affects pan and soil evaporation in the Negev Desert. *Ecohydrology* **9**: 1130-1138.

Formatiert: Englisch (USA)

Formatiert: Englisch (USA)

- 630 Koschorreck, M., Y. T. Prairie, J. Kim, and R. Marce. 2021. Technical note: CO₂ is not like CH₄ - limits of and corrections to the headspace method to analyse pCO₂ in fresh water. *Biogeosciences* **18**: 1619-1627.
- 635 Legendre, L., S. Demers, C. M. Yentsch, and C. S. Yentsch. 1983. The C-14 Method - Patterns of Dark CO₂ Fixation and DCMU Correction to Replace the Dark Bottle. *Limnol. Oceanogr.* **28**: 996-1003.
- Leyer, I., and K. Wesche. 2007. *Multivariate Statistik in der Ökologie. Eine Einführung.* Springer.
- Ma, J., Z.-Y. Wang, B. A. Stevenson, X.-J. Zheng, and Y. Li. 2013. An inorganic CO₂ diffusion and dissolution process explains negative CO₂ fluxes in saline/alkaline soils. *Sci Rep-Uk* **3**: 2025.
- 640 Machado dos Santos Pinto, R., G. Weigelhofer, E. Diaz-Pines, A. Guerreiro Brito, S. Zechmeister-Boltenstern, and T. Hein. 2020. River-floodplain restoration and hydrological effects on GHG emissions: Biogeochemical dynamics in the parafluvial zone. *Sci Total Environ* **715**: 136980.
- Macpherson, G. L. 2009. CO₂ distribution in groundwater and the impact of groundwater extraction on the global C cycle. *Chemical Geology* **264**: 328-336.
- 645 Mallast, U., M. Staniek, and M. Koschorreck. 2020. Spatial upscaling of CO₂ emissions from exposed river sediments of the Elbe River during an extreme drought. *Ecohydrology* **13**.
- Marcé, R. and others 2019. Emissions from dry inland waters are a blind spot in the global carbon cycle. *Earth-Sci. Rev.* **188**: 240-248.
- Martinsen, K. T., T. Kragh, and K. Sand-Jensen. 2019. Carbon dioxide fluxes of air-exposed sediments and desiccating ponds. *Biogeochemistry*.
- 650 Matoušů, A., M. Rulík, M. Tušer, A. Bednařík, K. Šimek, and I. Bussmann. 2019. Methane dynamics in a large river: a case study of the Elbe River. *Aquat. Sci.* **81**: 12.
- Musolf, A. and others 2021. Spatial and Temporal Variability in Concentration-Discharge Relationships at the Event Scale. *Water Resources Research* **57**: e2020WR029442.
- 655 Ohmori, M., S. Miyachi, K. Okabe, and S. Miyachi. 1984. Effects of Ammonia on Respiration, Adenylate Levels, Amino-Acid Synthesis and Co₂ Fixation in Cells of *Chlorella-Vulgaris* 11h in Darkness. *Plant and Cell Physiology* **25**: 749-756.
- Oikawa, P. Y., D. A. Grantz, A. Chatterjee, J. E. Eberwein, L. A. Allsman, and G. D. Jenerette. 2014. Unifying soil respiration pulses, inhibition, and temperature hysteresis through dynamics of labile soil carbon and O₂. *Journal of Geophysical Research: Biogeosciences* **119**: 521-536.
- 660 Palmia, B., S. Leonardi, P. Viaroli, and M. Bartoli. 2021. Regulation of CO₂ fluxes along gradients of water saturation in irrigation canal sediments. *Aquat. Sci.* **83**: 18.
- Penman, H. L. 1948. Natural Evaporation from Open Water, Bare Soil and Grass. *Proc R Soc Lon Ser-A* **193**: 120-&.
- 665 Perkins, A. K., I. R. Santos, M. Sadat-Noori, J. R. Gatland, and D. T. Maher. 2015. Groundwater seepage as a driver of CO₂ evasion in a coastal lake (Lake Ainsworth, NSW, Australia). *Environmental Earth Sciences* **74**: 779-792.
- Peters, E., G. Bier, H. A. J. van Lanen, and P. J. J. F. Torfs. 2006. Propagation and spatial distribution of drought in a groundwater catchment. *Journal of Hydrology* **321**: 257-275.
- 670 Phillips, C. L., N. Nickerson, D. Risk, and B. J. Bond. 2011. Interpreting diel hysteresis between soil respiration and temperature. *Global Change Biology* **17**: 515-527.

Formatiert: Englisch (USA)

Formatiert: Englisch (USA)

- R-Core-Team. 2016. R: A language and environment for statistical computing. R Foundation for Statistical Computing.
- Reichstein, M., F. Bednorz, G. Broll, and T. Kätterer. 2000. Temperature dependence of carbon mineralisation: conclusions from a long-term incubation of subalpine soil samples. *Soil Biol. Biochem.* **32**: 947-958.
- 675 Rey, A. 2015. Mind the gap: non-biological processes contributing to soil CO₂ efflux. *Global Change Biology* **21**: 1752-1761.
- Riveros-Iregui, D. A. and others 2007. Diurnal hysteresis between soil CO₂ and soil temperature is controlled by soil water content. *Geophys Res Lett* **34**.
- 680 Schlesinger, W. H., and J. M. Melack. 1981. Transport of organic carbon in the world's rivers. *Tellus* **33**: 172-187.
- Scholten, M. and others 2005. The River Elbe in Germany - present state, conflicting goals, and perspectives of rehabilitation. *Archiv für Hydrobiologie Suppl.* **155**: 579-602.
- Spinoni, J., J. V. Vogt, G. Naumann, P. Barbosa, and A. Dosio. 2018. Will drought events become more frequent and severe in Europe? *International Journal of Climatology* **38**: 1718-1736.
- 685 Steward, A. L., D. von Schiller, K. Tockner, J. C. Marshall, and S. E. Bunn. 2012. When the river runs dry: human and ecological values of dry riverbeds. *Front. Ecol. Environ.* **10**: 202-209.
- Tufekcioglu, A., J. W. Raich, T. M. Isenhardt, and R. C. Schultz. 2001. Soil respiration within riparian buffers and adjacent crop fields. *Plant Soil* **229**: 117-124.
- 690 UNESCO/IHA. 2010. GHG Measurement Guidelines for Freshwater Reservoirs, p. 138. *In* J. A. Goldenfum [ed.]. UNESCO.
- von Schiller, D. and others 2014. Carbon dioxide emissions from dry watercourses. *Inland Waters* **4**: 377-382.
- Weigold, F., and M. Baborowski. 2009. Consequences of delayed mixing for quality assessment of river water: Example Mulde-Saale-Elbe. *Journal of Hydrology* **369**: 296-304.
- 695 Weise, L. and others 2016. Water level changes affect carbon turnover and microbial community composition in lake sediments. *FEMS Microbiol. Ecol.* **92**.
- Wood, W. W., and D. W. Hyndman. 2017. Groundwater Depletion: A Significant Unreported Source of Atmospheric Carbon Dioxide. *Earths Future* **5**: 1133-1135.
- 700 WSV. 2020. ELWIS. Wasserstände & Vorhersagen an schiffahrtsrelevanten Pegeln. Pegel Magdeburg-Strombrücke. Wasserstraßen- und Schifffahrtsverwaltung des Bundes (WSV) im Geschäftsbereich des Bundesministeriums für Verkehr und digitale Infrastruktur (BMVI).
- Yvon-Durocher, G. and others 2012. Reconciling the temperature dependence of respiration across timescales and ecosystem types. *Nature* **487**: 472-476.
- 705

Formatiert: Englisch (USA)

Formatiert: Englisch (USA)